

**AN *HP*-ADAPTIVE FINITE ELEMENT
PROCEDURE FOR FLUID-STRUCTURE
INTERACTION IN FULLY EULERIAN
FRAMEWORK**

MOHAMAD AIZAT BIN ABAS

UNIVERSITI SAINS MALAYSIA

2013

**AN *HP*-ADAPTIVE FINITE ELEMENT
PROCEDURE FOR FLUID-STRUCTURE
INTERACTION IN FULLY EULERIAN
FRAMEWORK**

by

MOHAMAD AIZAT BIN ABAS

**Thesis submitted in fulfilment of the requirements
for the degree of
Doctor of Philosophy**

May 2013

ACKNOWLEDGEMENT

I would like to express depth of gratitude to my supervisor Dr-Ing Razi Abdul-Rahman for his unrelenting efforts in guiding me throughout my PhD project. Many thanks also to the Dean, Professor Zaidi bin Mohd Ripin and the USM Mechanical Engineering support staffs for their help and advices in the management side.

Moreover, I am grateful of my wife and kids soothing support and understanding, without them my PhD would never had been completed. Also, thanks a lot to my dear friends who shared with me their experiences and feedbacks to ease the journey of my Phd. A heartwarming thanks also to Elmer Multiphysics FEM team for their insights and guidance into the computing capability of Elmer software.

Not to forget, special acknowledgements to the USM and Ministry of Higher Education (MOHE) for their financial support during the whole of my PhD project; thanks abundantly for these.

TABLE OF CONTENTS

Acknowledgement	i
Table of Contents	ii
List of Tables	vi
List of Figures	vii
List of Abbreviations	xv
List of Symbols	xvii
Abstrak	xxiii
Abstract	xxiv
CHAPTER 1 –Introduction	1
1.1 Problem Statements	8
1.2 Objectives	10
CHAPTER 2 –Literature Review	11
2.1 <i>hp</i> -adaptivity	11
2.2 <i>A posteriori</i> error estimator	16
2.3 Parallel <i>hp</i> -adaptivity	17
2.4 FSI framework: ALE, Eulerian and Lagrangian approach	18
CHAPTER 3 –FE Procedures for Fluid-Structure Interaction	22
3.1 Fluid model in Eulerian formulation	22
3.2 Fluid model in ALE formulation	23
3.3 Navier-Stokes equations: FE discretization	25
3.3.1 Viscous term	27
3.3.2 Pressure term	29
3.3.3 Body force term	29
3.3.4 Continuity equation	30
3.3.5 Combined matrix form	31

3.3.6	Convective term	31
3.3.6(a)	Picard Iteration	33
3.3.6(b)	Newton Iteration.....	33
3.4	Stabilization Method	35
3.4.1	Stabilization Method : Contribution to stiffness terms	36
3.5	Sequential coupling algorithm.....	40
3.5.1	Level set for interface tracking	41
3.6	Structure: ALE formulation.....	42
3.7	Structure: Eulerian	46
3.8	Structure: Construction of Newton Linearization	48
3.8.1	Weak form of Saint Venant Kirchhoff elasticity model an its consistent linearization	48
3.9	Steady State Structure: ALE and Lagrangian framework	53
3.10	Directional derivatives	54
3.10.1	Differentiation scheme: Automatic Differentiation	55
3.10.1(a)	Automatic differentiation in the ALE framework	56
3.10.1(b)	Directional derivatives in terms of displacement	59
3.10.1(c)	Directional derivatives in terms of velocity	60
3.10.1(d)	Directional derivatives in terms of pressure.....	61
3.10.1(e)	Directional derivatives in terms of pressure, velocity and displacement	61
3.10.2	Automatic differentiations in the Eulerian framework.....	62
3.10.2(a)	Directional derivatives in terms of displacement	65
3.10.2(b)	Directional derivatives in terms of velocity	66
3.10.2(c)	Directional derivatives in terms of pressure.....	67
3.10.2(d)	Directional derivative in terms of pressure, velocity and displacement	67
3.11	ALE: Deformation of the fluid domain	68

3.11.1	Deformation of fluid domain: matrix form	69
3.12	Full FSI equation	70
3.13	Stationary fluid structure interactions	73
3.14	Software implementation: Construction of matrices and solution vector	73
CHAPTER 4 –Parallel <i>hp</i> -adaptive implementation in FSI		77
4.1	General Approach to <i>h</i> - and <i>p</i> -adaptivity	77
4.1.1	<i>hp</i> -Adaptivity: Regular and irregular meshes	78
4.1.1(a)	Finite Element Space	78
4.1.1(b)	Regular and irregular mesh	79
4.1.2	High order finite elements	79
4.1.2(a)	Hierarchical shape functions	81
4.1.2(b)	Continuity of regular mesh.....	82
4.1.2(c)	Hierarchical shape functions for triangles	82
4.1.3	Mesh refinement technique - <i>h</i> -method	86
4.1.3(a)	Regular mesh refinement	87
4.1.4	<i>hp</i> -adaptivity: Data structure.....	91
4.1.5	A posteriori error estimator	92
4.1.5(a)	FSI <i>a posteriori</i> error estimation	95
4.1.6	<i>hp</i> -Adaptive Keypoint Strategy	97
4.1.7	<i>hp</i> -adaptivity with parallel architecture	97
4.1.7(a)	Parallel implementation	97
4.1.7(b)	Parallel implementation with <i>hp</i> -adaptivity	100
4.2	Software implementation: <i>hp</i> -adaptive implementation	100
4.2.1	High Order Elements	100
4.2.2	Numerical integration for High Order Elements	102
4.2.3	Higher order basis and element mappings.....	102
4.2.4	<i>hp</i> -adaptive keypoint strategy.....	103

4.3	Software implementation: Parallel run implementation	107
4.4	Preconditioned iterative method	108
CHAPTER 5 –Results and Discussion		109
5.1	Fluid in Cavity	109
5.1.1	Fluid in Cavity: Convergence of error and norm	110
5.2	Loaded Elastic Beam	115
5.2.1	Loaded Elastic Beam: Convergence of error and norm	116
5.3	Elastic Driven Cavity	120
5.3.1	Cavity: ALE vs Eulerian	121
5.3.2	Cavity: Comparison adaptive methods (Fluid)	126
5.3.3	Cavity: Comparison adaptive methods (Structure)	131
5.3.4	Cavity: Comparison adaptive methods (Computation time) ..	137
5.4	Backward-step with Flexible Bottom (BFS)	141
5.4.1	BFS: ALE vs Eulerian	141
5.4.2	BFS: Comparison serial and parallel	142
5.4.3	BFS: Comparison adaptive methods (Fluid)	142
5.4.4	BFS: Comparison adaptive methods (Structure)	147
5.4.5	BFS: Comparison adaptive methods (Computation time)	153
5.4.6	BFS: Comparison of <i>hp</i> -adaptivity on ALE and Eulerian framework	154
5.5	Fluid Flow Around an Elastic Beam	157
CHAPTER 6 –Conclusion		160
6.1	Contributions of this thesis	161
6.2	Future works	162
Bibliography		164
Bibliography		164

LIST OF TABLES

Table 4.1	Number of nodes associated with vertex, edge and bubble function	102
Table 5.1	Number of elements and DOF for fluid in cavity test case	110
Table 5.2	Number of elements and DOF for loaded elastic beam test case	117
Table 5.3	L2-norm displacement in the whole structure domain for $\mu_s = 0.05$	123
Table 5.4	L2-norm displacement in the whole structure domain for $\mu_s = 0.1$	123
Table 5.5	Reynolds number and type of flow for increasing velocity	157

LIST OF FIGURES

Figure 3.1	Lagrangian, Eulerian and ALE domains map [12]	24
Figure 3.2	Sequential Algorithm of Fluid Structure Interaction	40
Figure 3.3	Flowchart of fluid or structure solver subroutine. The white area indicates the flowchart of either fluid or structure formulation which is alterable while the grey area indicates built in features. The arrows denote the built in subroutines that is called if required. Source: [46]	76
Figure 4.1	Forced Refinement of neighbouring element [74]	80
Figure (a)	Irregular mesh with hanging node	80
Figure (b)	Forced refinement of neighbouring element.....	80
Figure 4.2	Examples of regular and irregular mesh [58]	80
Figure (a)	Regular triangular mesh	80
Figure (b)	Regular quadrilateral mesh	80
Figure (c)	Irregular triangular mesh with hanging nodes	80
Figure (d)	Irregular quadrilateral mesh with hanging nodes	80
Figure 4.3	Maximum and minimum rule continuity requirement of triangular element hierachical shape function. The dotted line represents third order shape function of element K_2 [58]	83
Figure 4.4	Standard Triangular Element [84]	84
Figure 4.5	Triangle Vertex Functions. Source: [84]	85
Figure 4.6	Triangle edge functions. Source: [84]	86
Figure (a)	Second order edge function	86
Figure (b)	Third order edge function	86
Figure (c)	Fourth order edge function	86
Figure (d)	Fifth order edge function	86
Figure 4.7	Triangle bubble functions. Source: [84]	87
Figure (a)	Second, third and fourth order bubble function.....	87

Figure (b)	Fifth order bubble function.....	87
Figure 4.8	Red, Green, Blue Refinement criteria [87]	88
Figure 4.9	Forced refinement rules. Element 1 refers to the first marked element and Element 2 is the neighbouring element with forced refinement [95]	89
Figure (a)	Red refinement of Element 2 introduces two extra marked edge	89
Figure (b)	Blue refinement of Element 2 introduces one extra marked edge	89
Figure 4.10	Spatial Quad-Tree implementation with triangular elements [83]	90
Figure (a)	Parent elements	90
Figure (b)	1st level refinement. Light gray coloured elements indicate newly refined element belonging to the white coloured elements	90
Figure (c)	2nd level refinement. Dark gray coloured elements represents newly refined element belonging to the light coloured elements	90
Figure 4.11	Quad-Tree representation. First level tree is the parent element in white and subsequent level in light gray is the first leaf and dark gray second leaf.	91
Figure 4.12	Parallel computation with Domain Decomposition. Source: [46]	98
Figure 4.13	Partitioned FSI mesh into 4 cores using DD method. Bottom part is the structure domain and upper part is the fluid domain	99
Figure (a)	Initial mesh	99
Figure (b)	First parallelized mesh	99
Figure (c)	Second parallelized mesh	99
Figure (d)	Third parallelized mesh	99
Figure (e)	Fourth parallelized mesh.....	99
Figure 4.14	Parallel <i>hp</i> -adaptive scheme	101
Figure 4.15	Mismatched edge function of the shared edge. Source: [67]	103

Figure 4.16	The global direction of edge	103
Figure 4.17	h -adaptive refinement strategy with angle checking	106
Figure (a)	First level refinement without neighbouring element	106
Figure (b)	Second level green refinement with first neighbouring level angle $\geq 50^\circ$	106
Figure (c)	Second level red refinement with first neighbouring angle $\leq 50^\circ$. Green refinement on second neighbouring angle $\geq 50^\circ$	106
Figure (d)	Second level red refinement with first neighbouring angle $\leq 50^\circ$. Blue refinement on second neighbouring angle $\leq 50^\circ$	106
Figure 5.1	Fluid test with high order elements	110
Figure 5.2	Residual error indicator convergence for $p= 1, 2, 3$ with increasing DOF	111
Figure 5.3	Velocity norm convergence for $p= 1, 2, 3$ with increasing DOF	111
Figure 5.4	Velocity stream function of $V = 4x(1 - x)$ for fluid in cavity testcase	112
Figure 5.5	Velocity profile of fluid in cavity test case	112
Figure 5.6	Velocity magnitude for $p= 1, 2, 3$ on 200 elements	113
Figure (a)	1st order fluid test case	113
Figure (b)	2nd order fluid test case	113
Figure (c)	3rd order fluid test case.....	113
Figure 5.7	Pressure magnitude for $p= 1, 2, 3$ on 200 elements	114
Figure (a)	1st order fluid test case	114
Figure (b)	2nd order fluid test case	114
Figure (c)	3rd order fluid test case.....	114
Figure 5.8	Loaded Elastic Beam	116
Figure 5.9	Residual error indicator convergence for $p= 1, 2, 3$ with increasing DOF	116
Figure 5.10	Displacement norm convergence for $p= 1, 2, 3$ with increasing DOF	117

Figure 5.11	Displacement magnitude for for $p= 1, 2, 3$ on 120 elements	118
Figure (a)	1st order elasticity test case	118
Figure (b)	2nd order elasticity test case	118
Figure (c)	3rd order elasticity test case.....	118
Figure 5.12	Deformation of structure elasticity test case	119
Figure 5.13	Elastic Driven Cavity	120
Figure 5.14	Comparison of ALE and Eulerian framework on elastic driven cavity testcase with $\mu = 0.05$	122
Figure 5.15	Comparison of ALE and Eulerian framework on elastic driven cavity testcase with $\mu = 0.1$	122
Figure 5.16	Interface displacement for maximum parabolic velocity $v_{par}=1,2,3$	125
Figure (a)	Interface movement for $v=1$ magnified by 10^2	125
Figure (b)	Interface movement for $v=2$	125
Figure (c)	Interface movement for $v=3$	125
Figure 5.17	Convergence of residual error indicator for different adaptive methods on fluid solver	127
Figure 5.18	Convergence of norm for different adaptive methods on fluid solver	127
Figure 5.19	hp - and h - adapt on Cavity test case: Original mesh. The circle shape marker represents the key points associated with hp -adaptivite strategy	128
Figure 5.20	hp -adapt on Cavity test case: Fluid domain	129
Figure (a)	1st level fluid hp -adapt.....	129
Figure (b)	3rd level fluid hp -adapt	129
Figure (c)	7th level fluid hp -adapt	129
Figure (d)	12th level fluid hp -adapt	129
Figure 5.21	h -adapt on Cavity test case: Fluid domain	130
Figure (a)	1st level fluid h -adapt	130
Figure (b)	3rd level fluid h -adapt	130

Figure (c)	5th level fluid h -adapt	130
Figure (d)	7th level fluid h -adapt	130
Figure 5.22	Comparison of error for different adaptive methods on structure solver	131
Figure 5.23	Comparison of norm for different adaptive methods on structure solver	132
Figure 5.24	hp -adapt on Cavity test case: Structure domain	133
Figure (a)	1st level structure hp -adapt	133
Figure (b)	3rd level structure hp -adapt	133
Figure (c)	7th level structure hp -adapt	133
Figure (d)	12th level structure hp -adapt	133
Figure 5.25	h -adapt on Cavity test case: Structure domain	134
Figure (a)	1st level fluid h -adapt	134
Figure (b)	3rd level fluid h -adapt	134
Figure (c)	5th level fluid h -adapt	134
Figure (d)	7th level fluid h -adapt	134
Figure 5.26	Initial solution on a coarse mesh	135
Figure (a)	Displacement vectors.....	135
Figure (b)	Velocity vectors.....	135
Figure (c)	Pressure vectors	135
Figure (d)	Velocity profile and FSI interface displacement	135
Figure 5.27	12th level hp -adaptive solution on a finer mesh with maximum order=7 and minimum order=1	136
Figure (a)	Displacement vectors.....	136
Figure (b)	Velocity vectors.....	136
Figure (c)	Pressure vectors	136
Figure (d)	Velocity profile and FSI interface displacement	136

Figure 5.28	Comparison of computation time for different adaptive methods	138
Figure 5.29	Relative speedup of parallel implementation	139
Figure 5.30	Total computation time of parallel implementation with increasing number of processor	139
Figure 5.31	Relative efficiency of parallel implementation with increasing number of processor	140
Figure 5.32	Backward-step with Flexible Bottom	141
Figure 5.33	Comparison of ALE and Eulerian framework on BFS test case for increasing DOF	142
Figure 5.34	Comparison between parallel and serial solver on CentOS HPC	143
Figure 5.35	<i>hp</i> - and <i>h</i> - adapt on BFS test case: Original mesh with key points	143
Figure 5.36	Comparison of fluid error convergence on <i>hp</i> , <i>h</i> and normal refinement	144
Figure 5.37	Comparison of fluid norm on <i>hp</i> , <i>h</i> and normal refinement	144
Figure 5.38	<i>hp</i> -adapt on BFS test case: Fluid domain	145
Figure (a)	1st level fluid <i>hp</i> -adapt	145
Figure (b)	3rd level fluid <i>hp</i> -adapt	145
Figure (c)	4th level fluid <i>hp</i> -adapt	145
Figure (d)	7th level fluid <i>hp</i> -adapt	145
Figure 5.39	<i>h</i> -adapt on BFS test case: Fluid domain	146
Figure (a)	1st level fluid <i>h</i> -adapt	146
Figure (b)	2nd level fluid <i>h</i> -adapt	146
Figure (c)	3rd level fluid <i>h</i> -adapt	146
Figure 5.40	Comparison of structure error convergence on <i>hp</i> , <i>h</i> and normal refinement	147
Figure 5.41	Comparison of structure norm on <i>hp</i> , <i>h</i> and normal refinement	148
Figure 5.42	<i>hp</i> -adapt on BFS test case: Structure domain	149

Figure (a)	1st level structure <i>hp</i> -adapt	149
Figure (b)	2nd level structure <i>hp</i> -adapt.....	149
Figure (c)	4th level structure <i>hp</i> -adapt	149
Figure (d)	7th level structure <i>hp</i> -adapt	149
Figure 5.43	<i>h</i> -adapt on BFS test case: Structure domain	150
Figure (a)	1st level structure <i>h</i> -adapt	150
Figure (b)	2nd level structure <i>h</i> -adapt	150
Figure (c)	3rd level structure <i>h</i> -adapt	150
Figure (d)	4th level structure <i>h</i> -adapt	150
Figure 5.44	Initial solution on a coarse mesh	151
Figure (a)	Displacement vectors.....	151
Figure (b)	Velocity vectors.....	151
Figure (c)	Pressure vectors	151
Figure (d)	Velocity profile and FSI interface displacement	151
Figure 5.45	7th level <i>hp</i> -adaptive solution on a finer mesh with maximum order=11 and minimum order=1	152
Figure (a)	Displacement vectors.....	152
Figure (b)	Velocity vectors.....	152
Figure (c)	Pressure vectors	152
Figure (d)	Velocity profile and FSI interface displacement	152
Figure 5.46	Comparison of computation time on <i>hp</i> , <i>h</i> and normal refinement for parallel and serial solver	153
Figure 5.47	Comparison of fluid's residual error indicator of <i>hp</i> -adaptive method for ALE and Eulerian framework	154
Figure 5.48	Comparison of fluid's norm of <i>hp</i> -adaptive method for ALE and Eulerian framework	155
Figure 5.49	Comparison of structure's error of <i>hp</i> -adaptive method for ALE and Eulerian framework	155

Figure 5.50	Comparison of structure's norm of <i>hp</i> -adaptive method for ALE and Eulerian framework	156
Figure 5.51	Comparison of ALE and Eulerian computation time on <i>hp</i> and normal refinement	156
Figure 5.52	Fluid Flow Around Elastic Beam. Source: [47]	157
Figure 5.53	The velocity profile and beam displacement associated with increasing flow velocity from laminar to turbulent flow	159
Figure (a)	Velocity profile for laminar flow with maximum parabolic velocity 1. The displacement of the beam is multiplied by 10^2 for ease of view.....	159
Figure (b)	Velocity profile for laminar flow with maximum parabolic velocity 10	159
Figure (c)	Velocity profile for turbulent flow with maximum parabolic velocity 110	159

LIST OF ABBREVIATIONS

lim limit

2D Two dimensional

3D Three dimensional

ALE Arbitrary Lagrangian Eulerian

BC Boundary Condition

BFS Backward-step with flexible bottom

BiCGStab Biconjugate Gradient Stabilized

DOF Degrees of Freedom

FEA Finite Element Analysis

FEM Finite Element Method

FSI Fluid-Structure Interaction

GLS Galerkin Least Square

HPC High Performance Computer

ILU Incomplete LU

LS Level set

MFEM Meshless Finite Element Method

NEL Number of elements

NH Neo-Hookean material model

NH – ALE Combination of NH material model and ALE framework

NH – Eulerian Combination of NH material model and Eulerian framework

PK1 First Piola-Kirchhoff stress tensor

PK2 Second Piola-Kirchhoff stress tensor

Re Reynolds number

RHS Right Hand Side

RGB Red-Green-Blue

STVK Saint Venant Kirchoff material model

STVK – ALE Combination of STVK material model and ALE framework

STVK – Eulerian Combination of STVK material model and Eulerian
framework

SPH Smoothed Particle Hydrodynamics

STDOfs Number of DOF on each structure's element

VOF Volume of fluid

LIST OF SYMBOLS

$A^{(e)}$ Elemental area contribution

\hat{A}'_{ALE} Directional derivative of ALE framework

A'_{Eul} Directional derivative of Eulerian framework

$B(\cdot, \cdot)$ Bilinear form

$C = F^T F$ Left Cauchy-Green strain tensor

\hat{C} Right Cauchy-Green strain tensor

dim dimension

$(\operatorname{div} F)_i = \sum_j \partial_j F_{ij}$ Divergence of tensor

$\operatorname{div} f = \sum_i \partial_i f_i$ Divergence of tensor and vector

\mathbf{D} Displacement vector

$D(x)$ Deformation function of points in the deformed domain

$\det(\cdot)$ Determinant of function

E^s Young Modulus

f Force term

F Deformation gradient

$(f, g) = \int f g dx$ L^2 inner product

$\|f\|_X^2 = (f, f)_X$ L^2 norm

g Neumann source term

h_k Element diameter

$H^1(\Omega)$ Sobolev space of first order

h_K Element size
 h_e Edge size
 J Determinant of the deformation gradient
 J_E Jump in $[\cdot]$ across edge, E
 K Stiffness matrix
 K^t Equilateral triangle
 $L^2(\cdot)$ Lebesgue space of square integrable functions
 L_f Test space for mass conservation equation
 $L(\cdot)$ Linear form
 L_i Vertex functions in x,y and z direction
mu Mesh velocity in x -direction
mv Mesh velocity in y -direction
MD1 Mesh displacement in x -direction
MD2 Mesh displacement in y -direction
 m_k Constant for calculation of stabilization parameter
 N_i Finite element basis functions
 $N_i^{i,j}$ Edge function in x,y and z direction
 N_i^0 Bubble function
 n Unit vector normal
 P Pressure
 p_a Atmospheric pressure

p_K	Element K polynomial order of shape functions
\mathbb{R}	Real number
R_m	Residual of momentum equation
R_c	Residual of continuity equation
Re_K	Stabilization parameter
R	Mean curvature
R_K	Local residual of the finite element solution with respect to the equilibrium equation
$R_{E,\Omega}$	Residual of jump in $[\cdot]$ taken over all edges, E
R_{E,Γ_N}	Residual with respect to boundary condition
$S^{(e)}$	Elemental boundary contribution
S^s	Second Piola Kirchhoff stress tensor
trA	Trace of matrix A
t	time
\bar{U}	Previous velocity
$u_{h,p}$	Total basis function
$u_{h,p}^v$	Nodal basis function
$u_{h,p}^e$	Edge basis function
$u_{h,p}^f$	Face basis function
$u_{h,p}^b$	Bubble basis function
V_f^0	Test space for momentum equation

V_f^D	Test space for momentum equation on the prescribed Dirichlet boundary
\mathbf{v}	Velocity vector
v_{par}	Parabolic velocity
x	Point in spatial domain
X	Point in material domain
$X_h(K)$	Finite element space of shape function on specific element, K
θ	angle in radian
Ω	Full domain
Ω_f	Fluid domain
Ω_s	Structure domain
Γ_i	Fluid-structure interface
$\hat{\Omega}$	Domain in initial configuration
ρ	Density
σ	Stress
ν	Kinematic viscosity
μ	Dynamic viscosity
ε, E	Green-Lagrange strain tensor
χ	Point in ALE reference domain
$\psi(X, t)$	Map of the material material to ALE reference configuration
$\phi(X, t)$	Map of material configuration to spatial configuration
$\hat{\phi}(\chi, t)$	Map from ALE refence domain to spatial domain

Ω_0	Domain in initial configuration
$\hat{\Omega}$	Domain in ALE configuration
δ	Stabilization parameter
τ	Stabilization parameter
γ	Surface tension coefficient
∇_s	Surface gradient operator
Σ_s	First Piola Kirchhoff stress tensor
λ^s	First Lamé constant
μ^s	Second Lamé constant
ν	Poisson ratio
$\frac{d}{d\epsilon}$	Gâteaux directional derivative
χ_f	Characteristic function of fluid domain
χ_s	Characteristic function of structure domain
$\xi^i \nu^i$	Set of monomials
τ_D	Dirichlet boundary
τ_N	Neumann boundary
∇	Gradient of a function
$\eta_{R,K}$	Total element error indicator
η_K	Error indicator of local of the finite element solution with respect to the equilibrium equation
$\eta_{E,\Omega}$	Error indicator based on residual of jump in $[\cdot]$ taken over all edges, E

η_{E,Γ_N} Error indicator based on residual with respect to boundary condition

∂ Partial

∂_i Partial derivative of function with respect to i -th coordinate

∂_t Partial derivative of function with respect to time derivative

$(\nabla v)_{ij} = \partial_j v_i$ Gradient of a vector valued function v

$\frac{Df}{Dt}$ Material time derivative

w_i Referential particle velocity in x , y and z directions

$\partial_t u$ Partial time derivative

$[\cdot]$ Jump of a function across interior boundary

\cdot Dot product

\subset Subset

\in in

Tatacara Unsur Terhingga Ubahsuai- hp Bagi Interaksi Bendalir-Struktur Di Dalam Kerangka Penuh Eulerian

ABSTRAK

Tesis ini cuba melaksanakan prosedur kaedah unsur terhingga ubahsuai- hp sepenuhnya secara automatik bagi menyelesaikan masalah interaksi bendalir-struktur (FSI) dalam dua dimensi. Keberkesanan rangka penuh Eulerian pada FSI menggunakan ubahsuai- hp yang bergantung kepada ralat-*a posteriori* dan ubahsuai untuk mengurangkan ralat dalam norma tenaga juga dihipotesis. Adaptasi jaringan elemen secara automatik ke atas elemen segitiga dikendalikan melalui kaedah penghalusan merah-hijau-biru. Isu strategik ubahsuai jaringan elemen yang berkesan bagi mengelakkan peningkatan element berlebihan juga ditangani. Disebabkan kaedah ubahsuai- hp menggunakan kuasa polinomial tinggi sebagai fungsi penghampiran, sistem matrik yang terhasil adalah hampir penuh membawa kepada konsep pengiraan FSI secara selari. Pengiraan ubahsuai hp selari dinilai dengan ubahsuai seragam dan h yang konvensional pada beberapa kes ujian standard. Seterusnya, keberkesanan rangka penuh Eulerian berbanding kaedah terkenal iaitu Arbitrary Lagrangian Eulerian (ALE) juga dibandingkan menggunakan dua model bahan berbeza, iaitu, model St. Venant Kirchoff dan Neo-Hookean. Didapati bahawa rangka penuh Eulerian memberikan ramalan bendalir-struktur yang tepat untuk deformasi besar tanpa perlu kerap menyediakan jaringan element baru. Kaedah ubahsuai- hp juga didapati pendekatan terbaik bagi mendapatkan penyelesaian yang tepat tanpa banyak tolak ansur dalam memori dan masa komputer. Integrasi dengan perkomputeran selari pula telah berjaya mengurangkan masa pengiraan sehingga dua magnitud berbanding penyelesaian secara bersiri. Bagi perbandingan antara ALE dan rangka penuh Eulerian, penyelesaian kiraan untuk semua kes ujian didapati hampir sama.

An hp -Adaptive Finite Element Procedure for Fluid-Structure Interaction in Fully Eulerian Framework

ABSTRACT

This thesis attempts to implement a fully automatic hp -adaptive finite element procedure for fluid-structure interaction (FSI) problems in two dimensions. This work hypothesizes the efficacy of Fully Eulerian framework of FSI in hp -adaptivity on an *a posteriori* error estimator and adaptation for minimization of error in energy norm. Automatic mesh adaptation over triangular elements is handled by red-green-blue (RGB) refinement method. An effective mesh adaptivity to avoid excessive growth of unknowns is also addressed. Since the hp -method uses high order polynomials as approximation functions, the resulting system matrices are less sparse leading to the notion of FSI computation with parallelism. The parallel hp -adaptive computation is assessed with the conventional uniform and h refinement on a number of benchmark test cases. Subsequently, the efficacy of the fully Eulerian framework is compared to the well known Arbitrary Lagrangian Framework(ALE) for two different material models, namely, the St. Venant Kirchoff and the Neo-Hookean models. It was found that the fully Eulerian framework provides accurate FSI predictions for large deformation without need of frequent remeshing. The hp -adaptive method was also found to be a viable approach in obtaining accurate solutions without much compromise in computer memory and time. Furthermore, the integration of parallelism is successful in reducing the computation time by up to two orders of magnitude relative to the serial solver. For the comparisons between the ALE and the fully Eulerian frameworks, the computed solutions in all test cases are observed to be in agreement with each other.

CHAPTER 1

INTRODUCTION

Multiphysics analysis of fluid-structure interactions(FSI) poses significant challenge since it intricately combine aspects in computational fluid dynamics and computational mechanics; both the latter and former are by themselves major areas of numerical simulations and active research are still being carried out for accurate predictions to the physical systems. Industrial applications of FSI include analysis of aeroelasticity, flutter as well as heat exchanger [35, 56, 100, 82]. In contrast, aside from engineering, substantial research in biomedical field keeps on growing at a fast pace; analyses of aneurysm in large arteries and of artificial heart valves [88, 97, 57, 92] are but of few examples.

The driving force for achieving accurate solution of FSI relies heavily on the performance of computing devices and given recent advances in high performance computing(HPC), computations of complex coupling of fluid-structure dynamics are achievable. The past few years have seen profound interest for faster computations of finite element analysis(FEA) software, and major finite element software including Abaqus and Ansys, have begun utilising parallelization including multi-core technology for faster computation time. In this thesis, an OpenMPI software is used as the multicore parallelization platform on a high performance computer having 400 cores, separated evenly in a 22 combined master and slave nodes.

Some researchers might argue that the inadequacy of computational devices can be remedied by optimization of the numerical methodology which includes development of smart automatic adaptive algorithms that alters the mesh quality during FSI computation. This is the so called adaptive finite element method that progressively modifies the initial coarse mesh to rapidly reduce discretization error

of the coarse mesh. This thesis attempts to solve the FSI problems using an hp -adaptive finite element method (hp -FEM), by exhaustively searching for elements with large error indicator and careful decision making algorithm to either refine the local elements (h) or to increase the element's polynomial order (p) [84, 18].

To drive the hp -adaptive method, an *a posteriori* error estimation is introduced. Since discretization error can be large, unpredictable and can deteriorate the numerical prediction, the *a posteriori* error estimator play a vital role to control the meshing, the choice of adaptive algorithms and the reliability of the computed solutions [9, 93].

Even with optimized adaptive algorithms, as the DOF increases in order of magnitudes higher, especially in three-dimensional problems, the need for parallelization becomes inevitable. Given the current implementation, the numerical problems to be explored could be complex and large covering coupled multi-physics problem which are the essence of FSI. In addition, solution of the FSI problem should lead to exponential rates of convergence, using fewer DOF compared to conventional uniform refinement, and most importantly cuts the cost of computation time to a minimum.

Aside from computational performance, complications arise in the setup of coupled dynamics: fluid is usually modelled in Eulerian coordinates as opposed to structure which is normally modelled in Lagrangian coordinates. In a Lagrangian setup, one observes the displacement $\hat{u}(\hat{x})$ of mass point $\hat{x} \subset \hat{\Omega}_s$ in the reference domain $\hat{\Omega}_s$. The advantage of Lagrangian formulation is that it allows an easy tracking of free surfaces and interfaces between different materials, however, it suffers from its inability to follow large distortions without recourse to frequent remeshing.

In contrast, in Eulerian coordinates, the deformation and trajectory of the

mass points is not a cause for concern, instead, the velocity $v(x)$ and pressure $p(x)$ in spacial points $x \in \Omega_f$ is observed, in which Ω_f represents the domain for fluid region. Computational mesh in Eulerian formulations is fixed and the continuum moves with respect to the grid. This allows for large distortions to take place, at the expense of precise interface definition and the resolution of flow details. Since the Eulerian approach describes the FSI interface in a fixed mesh, an additional function needs to be introduced to identify the position of the interface. The most notable interface marker functions are the Level-set method which detects the position of the free surface by solving for a marker function, ϕ . At the interface of FSI, the value of the marker function is $\phi = 0$, while regions inside the fluid domain have $\phi < 0$ and $\phi > 0$ for domain outside of fluid region.

The dissimilarity in coordinate formulation makes the setup of common variational formulation difficult. Such variational formulation is desirable and forms the foundation in approach of residual based error estimation and mesh adaptation [33]. In FSI, combination of both Eulerian and Lagrangian coordinates can be cumbersome. The fluid domain is itself time-dependent and would require deformation from the structure domain at the interface, whereas in structure, the fluid boundary values (velocity and normal stress) are needed to account for interactions from fluid to structure part. Both of this cases would require values from one to the other, leading to loss of accuracy and can be computationally costly. On account of this problem, a partitioned approached have been implemented (see for instance [91]); decouple the problem into fluid and structure parts, solve each equations separately on two separate solvers, and finally iterate the solution until it converges to the value that satisfies both fluid and structure part as well as interface conditions. This method however, does not formulate the FSI equation in a complete variational form [25]. The main advantage of partitioned approach is that the resulting equations are significantly smaller and generally better conditioned than the monolithic system [76]. The problem with this approach however, lies in ensuring the convergence and the stability of coupling

condition on the FSI interface.

In the monolithic approach, the complete system of nonlinear algebraic equations arising from the coupled discretization of the equation of motion in the fluid and structure domain are solved as a whole, typically using Newton's method. This approach also permits for better interface conditions as the interface is now treated as internal interface ensuring more robust modelling of FSI since any domain splitting errors have been removed. However, the disadvantage of this approach is significant when dealing with multi-field problem; different scaling of variables on the interface can lead to poorly conditioned system. In large scale applications, poorly conditioned systems can cause direct solvers to fail miserably while indirect solvers can be unstable. Subsequently, the iterative solvers have to be used in which the efficiency of the monolithic approach relies heavily on the sophisticated preconditioners. Moreover, implementation of global preconditioner and maintaining the state of the art schemes in each each solver is difficult to achieve, hence, it is unsuitable for applications in large scale problems, e.g. aeroelasticity, an area which partitioned approach seems more reliable [26].

Despite the common opinions that monolithic formulation is required for mesh adaptation, this thesis attempts to solve error estimation and mesh adaptation on partitioned approach, by separately solving for error estimators and mesh adaptation in each fluid and structure domain using its respective solver. The mesh adaptation is done alternately during the FSI computation so that improvement in discretization error covers both fluid and structure domain. The partitioned approach will be associated with common variational formulation as part of the prerequisite for a posteriori error estimation and mesh adaptation. To implement common variational form for both fluid and structure would require that both problems being described in one common coordinate system. To do this would require either fluid or structure coordinate to reside in its natural coordinate system, while the other is formulated in a transformed coordinate system.

Afterwards, all computations are done on the fixed reference domain and as part of the computation, the supplementary transformation T_f have to be computed at each time step. The partitioned and transformation approach to overcome the Euler-Lagrange discrepancy explicitly tracks the fluid structure interface by mesh adjustment and are generally referred to as “interface tracking” method in which both methods leave the structure problem in its natural Lagrangian setting.

Arbitrary Lagrangian Eulerian description is by far the most popular "interface tracking" method [25]. A range of ALE references can be found in [12, 22, 51, 21]. In ALE formulation, complementary unknown coordinate transformation function is introduced only in the fluid domain since the structure will remain in its natural coordinate system (Lagrangian). As Lagrangian coordinate system resides in the undeformed configuration, it is inevitable to introduce an appropriate transformation function from deformed reference configuration to undeformed initial configuration, $\Omega_f, T_f(t) : \Omega_f \rightarrow \hat{\Omega}_f$. Thereafter, the computation is done on the fixed reference domain and since the supplementary transformation function forms part of the computation of FSI interface conditions, it needs to be computed in each time step.

In the conventional modelling with structure in Lagrangian fashion while fluid in Eulerian, there is no moving fluid surface mesh to which one could couple the moving structural surfaces. However with the introduction of transformation functions, the fluid structure coordinates are rewritten in the same reference domain that is fixed in time. For the fluid field, ALE method is established that allows the fluid mesh to be attached to fluid structure interface $\hat{\Gamma}_i$ at all times. Conversely, in Fully Eulerian coordinates, the interface $\Gamma_i(t)$ moves through the mesh elements and interactions between interface occur at certain points $x \in \Omega$ only.

ALE combines the best attributes of both Lagrangian and Eulerian coordi-

nates, since freedom is given to the nodes of the computational mesh to either move with the continuum similar to Lagrangian coordinate or be held fixed in Eulerian manner, or, moved in an arbitrary fashion to enable continuous rezoning capability. This freedom in mesh movement allows for greater mesh distortion compared to pure Lagrangian description and better resolution than in pure Eulerian fashion. In spite of ALE's role in improving mesh distortion, the mesh can still degenerate as the mesh distortions hit its limit.

As an alternative, both the fluid and structure coordinates can be modelled in Fully Lagrangian framework. Applications of Lagrangian technique appears promising when studying problems characterized by large displacement of fluid structure interface and by a rapidly moving free surface, e.g. FSI inside safety valves for pressure reduction [3].

For the present project, a variant of ALE and Pure Lagrangian approach is discussed as introduced by Dunne [25] namely the Fully Eulerian coordinates. In contrast to ALE method, the Fully Eulerian method maintains the fluid equations in its natural coordinate(Eulerian) whereas the structure is transformed using the supplementary transformation function. This function will transform structure's Lagrangian coordinate from the undeformed initial configuration to deformed reference configuration, $\hat{T}_s(t) : \hat{\Omega}_s \rightarrow \Omega_s$. This will be discussed in detail in the following chapter.

In this thesis, loosely coupled partitioned fluid structure interaction scheme is introduced on parallel *hp*-adaptive method for modelling of various test problems. This thesis starts off with the description of the governing equations for partitioned FSI in both natural as well as the transformed coordinates. The FSI problem is derived on ALE and Eulerian framework on two different material models namely St. Venant Kirchoff and Neo-Hookean model. Computations of the problems discussed are carried out using an open-source finite element re-

search code [1,25-28]. The computations were all restricted to triangular elements only. Moreover, conventional stabilization method is applied to discretize the governing equation, Navier Stokes equation, of the fluid motion [30, 29]. Stabilization terms are added to the conventional Galerkin formulation of the Navier-Stokes equations. The linear systems arises from the linearization are solved iteratively at the expense of direct method since preconditioned iterative solver is more stable and generally have smaller equations and better conditioned [76]. On top of the partitioned FSI, hp -adaptivity is applied and is driven to converge in global error norm separately for fluid and structure domains. An *a posteriori* error estimator based on residual estimator is introduced as error indicator for selective selective hp -adaptive refinement. Furthermore, simple algorithm is introduced following the approach by Schober and Kasper [77] that decides between h - and p -refinements using the prescribed keypoints where singularities exist. The h -refinement of triangular elements is based on the red-green-blue refinement technique for bisections of the parent element. To reduce the computation time associated with large number of degrees of freedom, a parallel domain decomposition technique is used in tandem with hp -adaptivity [46].

The thesis is organized starting with the Problem statement and Objectives to be solved in Chapter 1. Subsequently, Chapter 2 explores the Literature Review of adaptive methods, *a posteriori* error estimation, adaptive method with parallelism and review on various frameworks associated with fluid-structure interactions. In Chapter 3, the formulation of FSI in Eulerian and ALE frameworks combined with implementation using STVK and NH material models are introduced along with some introduction in its coding implementation. Moreover, Chapter 4 gives some introduction in to hp -adaptivity with parallelism and the coding side of its implementation.

1.1 Problem Statements

The ALE method is a well known method to treat fluid structure interaction problem. However, since the ALE framework still inherits the mesh distortion features of Lagrangian framework, the mesh is inevitably bound to fail. Donea and Huerta [21] underlines that ALE method could minimize the problem that arises in the classical kinematic description, but is prone to fail if mesh distortion reaches its peak. Richter and Wick [70, 69] distinguish ALE and Eulerian method in term of the usage of transformation function. In the ALE method, the transformation function, T , is used to transform the flow domain and for large flow deformation, the ALE approach can break down since severe mesh deterioration can cause the determinant of deformation gradient, J to turn zero or mount up to infinity. In the Eulerian method, however, T is used to transform the structure domain which does not move severely as in the case of fluid flow. Therefore, T is regularly well defined and the possibility of J approaching zero or infinity is highly unlikely.

In modelling the *hp*-adaptivity with ALE framework, the moving boundary features of ALE globally distorts domain it moves into. In FSI formulation, mesh refinement is concentrated at the vicinity of FSI interface and the newly created triangular elements are usually comprises of nearly distorted elements. Hence, the probability of elements to fail due to mesh distortion caused by moving boundaries amplify significantly. This problem is sorted with the introduction of fully Eulerian framework for the whole FSI domain. The main attribute of Eulerian framework is that its mesh is fixed along with its ability to undergo large displacement without the need for frequent remeshing. This attributes is important for FSI formulation since the stability of converged FSI solution is highly sensitive to element's distortion.

To the best knowledge of the author, most publications involving adaptive

FSI involves the use of quadrilateral elements since it is easier to subdivide the elements and the problem with aspect ratio can be avoided. The trade off with quadrilateral elements however is its inability to model FSI problems involving complex geometry.

In addition, the existing formulation of NH includes contribution contribution of both pressure and displacement contributions which can be cumbersome and consumes extra computation time for processing of both pressure and displacement contributions. In contrast, the current formulation of NH uses Labelle's formulation that requires only contribution for displacement. For the STVK material model, same formulation is used with Dunne

Moreover, the implemented *hp*-adaptive keypoint strategy with FSI problems, managed to reduce the amount of DOF required to reach low error and accurate solutions. However, due to complexity of FSI test cases especially for problems involving many singularity points, huge amount of DOF is still required. It suffices to say that *hp*-adaptivity alone is not capable of reducing computational effort. With the parallel solver already available for use with existing software and the availability of HPC computer, the combination of both *hp* and parallel computation becomes easier to implement to further reduce computational time to a bare minimum. Extension from serial adaptivity to parallel adaptivity however, would represent major re-writing of the current serial solver code to parallelized version.

The combined features of parallel *hp*-adaptivity with Fully Eulerian framework is capable of solving complex FSI system with maximum efficacy. The computed solution is expected to give faster convergence rate within minimum number of DOF with further reduction in computational time and effort. This is inline with the main target of this thesis; to develop a procedure for accurate yet efficient finite element computation of FSI.

1.2 Objectives

- To develop a method for inclusion of the STVK and NH material models in the Fully Eulerian setting. The current implementation uses combination of STVK material model and ALE framework (ALE-STVK). Therefore, three new combinations namely Eulerian-STVK, ALE-NH and Eulerian-NH have been implemented to complement the current formulation. The Eulerian-STVK will follow formulation by Dunne, ALE-NH following Labelle's formulation and Eulerian-NH is derived by the author.
- To construct algorithms of h , p , and hp adaptivity in an existing FSI solver code.
- To develop a residual *a posteriori* error estimator for application of hp and h adaptivity for FSI on Fully Eulerian framework based on the three new combined formulations
- To assess the performance aspect of hp -adaptivity including parallel performance with h -adaptivity and uniform refinement method. Both ALE and Eulerian formulation using hp -adaptivity are tested on a test problem first established by Dunne *et. al.*

CHAPTER 2

LITERATURE REVIEW

2.1 *hp*-adaptivity

The finite element method is the most widely accepted multi-purpose technique for numerical solution in applied mathematics and engineering [53]. Its principal applications include fluid flow, continuum mechanics, thermodynamics and field theory. With enormous advances in computation power, the finite element method benefits strongly and multi-field problems involving interactions between different nature i.e. fluid-structure, fluid-acoustic or even fluid-structure-acoustic interaction can be modelled with relative ease.

A foundation for formulation of finite element mathematical model was derived by Galerkin [34] which is closely related to the variational principal by Ritz et. al. [72]. The term finite element method was then firstly introduced by Clough [15] after its mathematical model was formulated and proposed by Courant [16] with lack of attention given by researchers during that period. The name was introduced 5 years after its first engineering applications by Clough et. al. on structural problems [52]. Various books are available covering the formulation and derivation of finite element method [103, 87, 42, 11]. It is worth mentioning that Zienkiewicz and Taylor gives a comprehensive introduction and formulation of fluid structure interactions [103]. Donea and Huerta formulated FSI on ALE framework and give some illustrated applications of FSI problems for industry [22].

The finite element method however is prone to discretization error and the need to control the error is a necessity for reliable and fast convergent finite element solutions [85]. For the past 20 years, vast amount of researches conducted

to find optimal strategies to guarantee rapid convergence of error in computed problems [84]. Three types of refinement strategy have been explored up to date namely:

- h -refinement which refine or coarsen local mesh
- p -refinement which increase or decrease the polynomial order of the basis function
- r -refinement which involves relocation or moving the nodes to improve element's aspect ratio

In comparison, r -refinement is more suited with transient problems, however, r -refinement alone is unable to find solution with specified accuracy and if the mesh is too coarse achieving the required convergence is fairly difficult unless more elements is added and the polynomial order is increased. h -refinement is byfar the most used refinement method given its ability to augment convergence rate even with the presence of singularity. Likewise, p -refinement too can speed up convergence and in the case of smooth solution exponential rate of convergence is achievable. Despite this advantage, the downside is that p -refinement does not perform as well in the presence of singularities where solution is rather non-smooth. Furthermore, p -refinement introduces fully populated mesh that could increase the computational time substantially. Given that both h -refinement and p -refinement having their own advantageous and disadvantageous, optimized mesh can be achieved by combining both the h - and p - refinement. This is the well known hp -adaptive method.

The pioneering work for hp -adaptive method rooted back to the work by Szabo *et. al* [7, 87]. Based on his research, applying only p -adaptive method while fixing the mesh could give exponential rate of convergence given that the problem is simple, i.e. unit cubes with periodic boundary condition. In practice, achieving

such convergence requires the problem to be free of singularities that regularly present in corners and material interfaces. Huge amount of literatures have been attributed to finding the right the combination of h and p -adaptivity but in most cases it boils down to the whether non-smooth solution or singularities is present in the domain. Babuska and Vogelius found that in the absence of singularities where the solution is smooth, the rate of convergence for p -adaptive method is two times faster compared to h -adaptive method [96]. However, when the solution is non-smooth, the rate of convergence for p -method is the same as h -method when refinement is based on uniform mesh refinement[87].

Unlike the p -method, the h -method is independent of the smoothness of the solution and given that optimal or nearly optimal mesh is used the rate of convergence of h -method is equal to the p -method. It would be easy to just resort to the p -method, however, the main concern of the p -adaptive method is that it produces more densely populated matrices which proves to be major stumbling block in terms of computational storage [84]. Therefore, in finding the compromise between computational storage and problems relating to singularity, the hp -method is introduced. In this thesis, the h -method is preferred in regions where singularities are located, while to boost the rate of convergence, a p -adaptive method is applied elsewhere. In theory, it is expected that hp -FEM could produce fastest convergence of solution in a given error norm and generally achieves exponential rate of convergence, thereby producing accurate solution within smallest number of degrees of freedom (DOF) compared to conventional uniform refinement [87].

To the author's knowledge, efforts at using an adaptive FEM approach in FSI computations, in particular hp -FEM are still considerably scarce. Historically, the use of high order elements is concentrated on problems relating to solid mechanics application, however Dubiner [24] applied high order spectral method for simulation of Navier-Stokes equation in a periodic pipe. Following on his path, Schwab [78] gives a comprehensive discussion on p - and hp -adaptivity for appli-

cation on fluid and solid mechanics problems. Initial effort on hp -adaptivity with FSI is contributed on the work by Oden which investigate multiscale phenomena in FSI test case [58].

Recently, the work of Van der Zee which is also based on goal-oriented error estimator, and applied on a fluid domain in contact with elastic boundary rather than elastic domain [19]. The problem can be categorized as free boundary problems with the fluid part modelled using Stokes flow model and the elastic domain is formulated using low-order structure line or string model. The key contribution by Van der Zee is the formulation of FSI using domain map linearization approach in which the linearized dual problem is derived by taking into account the domain geometry of FSI problems. In terms of adaptivity, however, no particular attention is paid on application of the FSI problems using high order elements and only h -adaptive refinement method is used for application on a number of FSI problems.

Moreover, large amount of literature on FSI are based on interactions of fluid domain with fixed rigid structures [62, 4]. The hp -adaptive method based on *a posteriori* error estimator is applied to compute free vibrations of a bundle of tubes of various shapes being immersed in an incompressible fluid contained in a rigid cavity. In comparison to the current implementation in this thesis, h -refinement is conducted by only using Red refinement criteria where four new elements is introduced which sometimes might lead to excessive growth of h -refinement. Moreover, for the error indicator, comparison of the current local estimated error with a prediction of this error obtained from the preceding step to decide whether to proceed with h or p refinement. On the contrary, this thesis utilizes residual based *a posteriori* error estimator.

Furthermore, Fick et. al. applied fluid-structure problems on an adaptive time dependent finite element formulation [27]. The fluid is modelled using simplified

inviscid fluid and for the structure, its kinematic is modelled using Euler-Bernoulli beam. Goal-oriented adaptivity on h and hp method are applied to a set of FSI problems being analyzed using adjoint-consistent discretization. Based on their findings, tremendous savings in computational cost can be realized through the use of adjoint-consistent goal-oriented refinement strategies. The goal-oriented approach also successfully equilibrates the error contributions of the FSI problems.

In addition, Bengzon and Larson modelled the one-way coupling of stationary FSI problem on h -adaptive method [13]. The structure model is formulated using linear elasticity model and the fluid domain is modelled using Stokes flow. The paper however does not present any results with regards to efficiency of adaptive method with FSI problems.

Selim develop and analyze h -adaptive element method for fully coupled, time dependent FSI problems [80]. To drive the adaptive method, an *a posteriori* error estimator based on the solution of auxiliary linearized dual problem is solved to control the error in a given goal functional of interest. Selim also explored the use of operator splitting method in the computation of the FSI numerical solution. The fluid subproblem is solved using inconsistent splitting method while the structure and mesh subproblem are solved using pure Galerkin method. The FSI formulation is then tested on a number of test cases to demonstrate the efficiency of adaptive algorithm.

Substantial contributors also in this area of research are arguably made by Dunne and Rannacher, Richter and Wick who proposed goal-oriented h -adaptivity on FSI problems [25, 69]. Dunne *et. al.* investigated the monolithic formulation of FSI problems involving incompressible Newtonian fluid interacting with two different material models namely St. Venant Kichoff and Neo-Hookean material model. The formulation of Neo-Hookean material used in Dunne's formulation

makes use of both displacement and pressure contributions which can be cumbersome to solve. Labelle on the other hand introduces Neo-Hookean formulation that involves only contributions from displacement which in turn reduces the complexity of Neo-Hookean formulation [50]. Moreover, Dunne *et. al.* also focuses application of adaptive methods on quadrilateral which could be challenging to implement in complex shape geometry. Based on the knowledge of the author, evidently no attempt has been made by the group to implement their current adaptive FSI formulation on parallel architecture.

2.2 *A posteriori* error estimator

The term error estimator is usually distinguishable to two different types namely *a priori* and *a posteriori* error estimates; the former are based on some general information about the exact solution that is generally not known or known very inaccurately while the latter are based upon additional information from the finite element solution e.g. residual values or other computable quantities and this value is very accurate [87]. From the standpoint of engineering applications, the *a priori* error estimates make use of the information from the exact solution which is not identifiable for many real world applications leading to the need for proper constructions of *a posteriori* error estimators. The pioneers on the formulation of *a posteriori* error estimates for finite element methods was initially explored by Babuska [34, 6, 51]

An in-depth research for *a posteriori* error estimation has been done by Ainsworth and Oden and has found applications in a huge number of scientific programs and commercial softwares [1]. Segeth derived *a posteriori* error estimator for Navier-Stokes equation and linearized elasticity problem [79]. Zienkiewicz in his paper gives a detailed introduction on error estimators for application with various adaptive methods [102]. In this thesis, explicit error estimator is used that computes error indicator using residual value obtained for each element of

fluid's or structure's numerical formulation. In comparison to explicit error estimator, the implicit method are known to be more reliable in the presence of pollution, however they are proven to be costly as the polynomial order increases [77]. Likewise, the recovery method are unreliable for higher polynomial order and also unable to treat pollution effects [6]. For this reasons, the explicit method supersedes both methods in terms of treating high order system as long as the solution has high regularity and generally requires lesser amount of computation time. The drawback of explicit method however, is its inability to guarantee error bounds at corner singularities and does not recognize numerical phase lag in wave problems.

In this thesis, Melenk and Wohlmuth [55] error estimator that includes the effect of polynomial change in the calculation of local error estimation is applied. This is in contradiction to the ones given by Ainsworth and Oden [1] and Verfuth [94] that neglects the contribution of polynomial order in error estimator calculations. The new error indicator does not underestimate local error indicator and generally leads to graded mesh at region of singularities.

2.3 Parallel *hp*-adaptivity

Earliest efforts on parallel *hp*-adaptivity follow the work by Oden and Patra [59] as well as Devine and Flaherty [20]. Moreover, Paszynski and Demkowicz explored parallel *hp*-adaptivity for three dimensional application of Elliptic and Maxwell problems [64]. Following these efforts, application of Schur Complements on parallel *hp* adaptivity is done by Paszynski *et. al.* [65].

Recently Hron and Turek published a paper on ALE approach to monolithic FSI for application in biomechanics and highlights the importance of fast solver in solving very large linear systems involving fluid-structure interactions [40]. Hoffman *et. al.* implement parallel *h*-adaptivity on various three dimensional

model of monolithic FSI problem based on combination of ALE framework and Neo-Hookean material model [38].

Ballman *et. al.* tries to solve parallel h -adaptivity of FSI problems using partitioned FSI; the fluid domain is solved using Finite Volume Method while the structure is solved using Finite Element method [8]. In this paper a geometrical and load transfer between Finite Element method and Finite Volume method are constructed to satisfy the same energy balance as the continuous system. This sort of FSI formulation is capable of detecting wake vortices as far as some 100 wing spans behind airplane, which could be hazardous to the airplane being modelled. Therefore, the aim of Ballman's research is to induced instabilities into the system of vortices to accelerate their alleviation.

Interestingly, none of the above parallel adaptive methods tries to solve adaptivity using triangular elements. Based on the author's findings, the formulation of adaptivity of quadrilateral elements are relatively simpler, however, triangular elements are much better suited for application on problems having highly complex geometrical shape.

2.4 FSI framework: ALE, Eulerian and Lagrangian approach

In combining both Lagrangian and Eulerian formulation in a partitioned FSI setting requires tracking of FSI boundary for the fluid's spatial domain as a result of deformation in the structure domain. This process requires mesh update to ensure in the fluid domain to satisfy the boundary conditions altered during structure's deformation. Its possible to just move the mesh accordingly however without proper mesh update algorithm would result in poor mesh quality that affects the stability and convergence of the numerical FSI solutions. Given this fact, additional mesh update equation is introduced in the current FSI formulation to ensure stability and quality of the moving FSI boundary interface. A

well known numerical formulation to handle this sort of problem is the so called Arbitrary Lagrangian Eulerian (ALE) formulation. The work on ALE method dated back to initial work by Huerta and Liu by using ALE to study nonlinear viscous fluid under large free surface wave motion for applications on a dam-break and tsunami problem [41]. Among huge contributors for ALE with FSI problem is denoted on the work by Turek et. al. with a number of benchmarking test case proposed for FSI problems [89, 90, 91]. Rugonyi and Bathe [75], describes ALE formulation on a fully coupled fluid-structure interactions with some emphasize on stability analysis on the interface equations and choices of time integration schemes.

Alternatively, the FSI problem can be formulated on Fully Eulerian framework. In fully eulerian framework, since the material points move relative to fixed mesh, a phase variable is employed to distinguish between fluid and structure domains. This method is commonly known as “interface capturing” method. The Level Set(LS) method and the Volume of Fluid(VOF) is a example of such phase variable implementation. The former pioneered by Osher and Ethian [61] has been successfully employed to treat complex flow problems involving changes in topology, i.e. surface breakup and moving boundaries. In the LS method, the boundary of the interior fluid layer is tracked while in the VOF method, the motion of the interior region is tracked. The advantage of VOF method is that complicated topological are easily treated, however, it suffers from difficulty to accurately calculate the curvature [81]. For this reason, LS method is the preferable option due to its ability to accurately track the boundary of the fluid. Moreover, the LS method is capable of computing interface singularities, for instance, corners, merging and reconnection of surfaces [23]. The problem with LS method is that it is susceptible to numerical dissipation leading to poor mass conservation property [98]. This drawback however, is remedied by using reinitialization technique by keeping the level set as a distance function and enforcing mass conservation. Chang, Hou, Merriman and Osher implemented the LS method for

interface capturing of incompressible fluid flow problem [14]. Following this effort, Deiterding investigates the adaptive LS method on shock-driven FSI problem by employing finite volume as ghost shell and the interface of FSI is tracked using LS function, ϕ [17]. Sugiyama *et. al.* examines the numerical accuracy associated with modelling of LS method on FSI problems for NH, STVK and Mooney-Rivlin material models [86].

As an alternative, both the fluid and structure coordinates can be modelled in Fully Lagrangian framework. Applications of Lagrangian technique appear promising when studying problems characterized by large displacement of fluid structure interface and by a rapidly moving free surface e.g. FSI inside safety valves for pressure reduction [3]. In a Fully Lagrangian framework the convective terms can be omitted since the motions of individual particles are followed. As a result, the nodes can be viewed as moving particles or commonly called “Particle Method”. A large literature of fully Lagrangian formulation is available for reference; refer [60] for particle method method with Smoothed Particle Hydrodynamic (SPH) and [44, 101] for particle method with Meshless Finite Element Method (MFEM). The disadvantage of particle method lies in the necessity of frequent mesh regeneration and efficiently moving the mesh nodes.

The formulation of mass conservation and momentum equation to model solid and structure is insufficient to give good distinction between one solid material to the other or from one type of fluid to the other. For this reason, different constitutive laws are constructed depending on the type of material e.g. elastic or hyperelastic model for the structure domain. The mathematical model to formulate material behaviour ensures accurate modelling of fluid and structure interaction which is problem specific. The commonly used constitutive equation to model hyperelastic structure are the St. Venant Kirchhoff and Neo-Hookean material model. A comprehensive insight into the two constitutive laws for hyperelastic materials can be found in [12, 43, 36, 39]. For the fluid domain, it is modelled

using the so called Navier Stokes equations and for this thesis the incompressible assumption is incorporated for ease of FSI modelling. Complete coverage of fluid modelling using Navier Stokes equation can be found in [22, 63, 99]

CHAPTER 3

FE PROCEDURES FOR FLUID-STRUCTURE INTERACTION

3.1 Fluid model in Eulerian formulation

For the rest of this section, the derivations of FSI on ALE and Eulerian using two different material models, St. Venant Kirchhoff and Neo-Hookean material models is followed closely as given by Dunne et al [33]. Note that common symbols are referred to the list of symbols since some may not be defined in the following chapter.

For the fluid, a Newtonian incompressible fluid is observed governed by the equations based on the conservation of mass and momentum. The equations are set in an Eulerian framework in the time-dependent domain $\Omega_f(t)$ with the pressure field $p_f \in L_f$ and the velocity vector field $v_f \in v_f^D + V_f^D$ as the variables. Here v_f^D is a suitable extension of the prescribed Dirichlet data on the boundaries (both moving or stationary) of $\Omega_f(t)$, and g_1 is a suitable extension to all of $\partial\Omega_f$ of the Neumann data for $\sigma_f \cdot n$ on the boundaries.

The variational form of the Navier Stokes equations in an Eulerian framework is obtained by multiplying them with suitable test functions, ψ from the test space V_f^0 for the momentum equation and L_f for the mass conservation equation. The equation in the variational form is written as:

Find $[v_f, p_f] \in [v_f^D + V_f^0] \times L_f$, such that $v_f(0) = v_f^0$, and

$$\left(\rho \frac{\partial v}{\partial t} + \rho(v \cdot \nabla)v, \psi\right) + (\nabla \cdot \sigma, \psi) = (g_1, \psi)_{\partial\Omega} + (f_1, \psi), \quad (3.1)$$

$$(\operatorname{div}(v), \psi) = 0. \quad (3.2)$$

for all $[\psi^v, \psi^p] \in V_f^0 \times L_f$, where

$$\begin{aligned}\sigma_f &= -pI + 2\rho_f\nu_f\varepsilon(v) \\ \varepsilon(v) &= \frac{1}{2}(\nabla v + \nabla v^T)\end{aligned}$$

Eq. 3.1 and 3.2 is the variational form of the Navier-Stokes equations.

3.2 Fluid model in ALE formulation

To derive the fluid's model in ALE framework [12], consider the problem governed by the incompressible Navier-Stokes equations

$$\left(\rho \frac{\partial v}{\partial t} + \rho(v \cdot \nabla)v, \psi \right) + (\nabla \cdot \sigma, \psi) = (g_1, \psi)_{\partial\Omega} + (f_1, \psi), \quad (3.3)$$

$$(\operatorname{div}(v), \psi) = 0. \quad (3.4)$$

The ALE framework requires description of **motion of the mesh** and **material motion**. The motion of the material is given by a function of material coordinate, X

$$x = \phi(X, t) \quad (3.5)$$

which maps the body in the initial configuration Ω_0 to the current or spatial configuration Ω . Figure 3.1 depicts the relationship between ALE coordinate to the spatial and material coordinates.

As shown in Figure 3.1, the ALE framework introduces *referential* domain $\hat{\Omega}$ that is also called ALE domain. Therefore, the motion of the mesh can be described as a function of ALE map as follow:

$$x = \hat{\phi}(\chi, t), \quad (3.6)$$

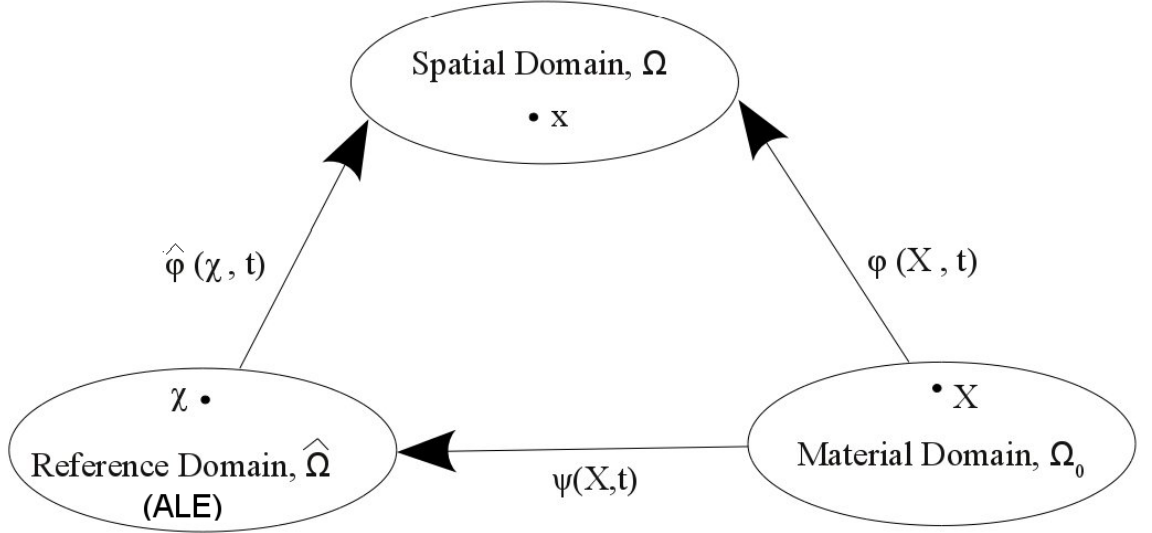


Figure 3.1: Lagrangian, Eulerian and ALE domains map [12]

where the ALE domain describes the motion of the mesh independent from the material motion. The map $\hat{\phi}$ plays a pivotal role in the derivation of finite element problem in ALE framework since it maps point x in the spatial or deformed domain to the point χ in the ALE domain. Consider a function $f(\chi, t)$ and using the chain rule, the material time derivative in ALE framework is defined as

$$\frac{Df}{Dt} = \frac{\partial f(\chi, t)}{\partial t} + \frac{\partial f(\chi, t)}{\partial \chi_i} \frac{\partial \psi_i(X, t)}{\partial t} \quad (3.7)$$

where the referential particle velocity w_i is given as

$$w_i = \frac{\partial \Psi_i(X, t)}{\partial t} = \frac{\partial \chi_i}{\partial t} \Big|_X \quad (3.8)$$

and finally after substitution of Eq. (3.8) in to (3.7) will give the following expression:

$$\frac{Df}{Dt} = \frac{\partial f}{\partial t} + \frac{\partial f}{\partial \chi_i} w_i \quad (3.9)$$

Notice that in general $w_i(X, t) = v(X, t)$ in which v representing material velocity. However, two particular cases can be distinguished: